

Crystallization of Rhenium Salts in a Simulated Low-Activity Waste Borosilicate Glass

Brian J. Riley,^{*,†} John S. McCloy,^{*} Ashutosh Goel, Martin Liezers, Michael J. Schweiger, Juan Liu, Carmen P. Rodriguez, and Dong-Sang Kim

Pacific Northwest National Laboratory, PO Box 999, Richland, Washington 99352

This study presents the characterization of salt phases that formed on simulated low-activity waste glass melts during a rhenium solubility study. This study with rhenium salts is also applicable to real applications involving radioactive technetium salts. In this synthesis method, oxide glass powder is mixed with the volatile species, vacuum-sealed in a fused quartz ampoule, and then heated in a furnace. This technique restricts the volatile species to the headspace above the melt but still within the sealed ampoule, thus maximizing the concentration of these species that are in contact with the glass. Above the previously determined solubility of Re^{7+} in this glass, a molten salt phase segregated to the top of the melt and crystallized into a solid layer. This salt was analyzed with X-ray diffraction, scanning electron microscopy, energy dispersive spectroscopy, as well as wavelength dispersive spectroscopy and was found to be composed of alkali perrhenates (NaReO_4 , KReO_4) and alkali sulfates. Similar crystalline inclusions were found in the bulk of some glasses as well.

I. Introduction

VITRIFICATION is the planned technology to immobilize the low-activity radioactive waste (LAW) stored at the Hanford site in Washington State. This waste is a byproduct of 45 years of plutonium production and currently occupies $2.1 \times 10^{11} \text{ m}^3$ in underground tanks. Within these tanks are elements that span the periodic table, some of which are long-lived isotopes with half-lives ($t_{1/2}$) lasting for hundreds of thousands to millions of years, most notably technetium-99 (^{99}Tc , $t_{1/2} = 2.1 \times 10^5 \text{ yr}$) and iodine-129 (^{129}I , $t_{1/2} = 1.6 \times 10^7 \text{ yr}$). The Hanford site tanks contain an estimated $\sim 9 \times 10^2 \text{ TBq}$ ($\sim 1500 \text{ kg}$) of ^{99}Tc and $\sim 1 \text{ TBq}$ ($\sim 180 \text{ kg}$) of ^{129}I .¹ Current calculations estimate that $>90\%$ of the ^{99}Tc inventory and 20% of the ^{129}I inventory in the tanks will be immobilized in the LAW glass.²

Technetium is a problematic component in glass for several reasons. Pertechnetate (TcO_4^-) and TcO_2 are the primary forms of Tc present in glass and are at least somewhat soluble in water, although TcO_2 is much less so.^{3,4} Thus, if released, the Tc will migrate easily into the ground water.^{5,6} Also, Tc-species are volatile so the Tc retention during the vitrification process tends to be low.^{3,7–9} Although it is not preferred, this lost fraction can be captured with off-gas scrubbing and recycled back into the process loop.

Technetium volatilization can be higher when preferentially segregated into a molten salt phase, if present, and Kim *et al.*⁹ noted that this is more probable when in the

presence of sulfates. It is well-known that sulfates are a cause of concern during melting as are other anionic salts (e.g., NO_2^- , NO_3^- , Cl^- , I^- , CrO_4^{2-}) present in LAW.^{10–14} This is because a layer of salt, sometimes called “gall”, is formed on the melt pool surface.¹⁵ This gall layer is fed by molten inclusions of salt that have a lower viscosity and density than the melt and tend to float to the top of the melt where they remain segregated or are reduced (such as $\text{SO}_4^{2-} \rightarrow \text{SO}_2$) and leave the melt (i.e., volatilize) as a gas. This behavior is a result of these anions being present in depolymerized regions of the melt where they segregate out of the polymerized glassy regions during cooling.^{16–19} Some of the primary limitations to retention are the Tc solubility and volatility in the selected base glass, which will change with glass composition.

The ultimate goal of this study was to determine the solubility of Tc in a borosilicate glass for vitrification of Hanford LAW, but rhenium (Re^{7+}) was used as a Tc surrogate to develop the technique. Rhenium is the most commonly selected Tc surrogate for waste glass applications because it is the most similar in chemistry, ionic size, and speciation in glass.³ The most common form of Tc found in the LAW simulants, as well as the liquid and vapor phases during vitrification, is Tc^{7+} , e.g., KTcO_4 , Tc_2O_7 .³ Thus, the species selected for this study were KReO_4 and Re_2O_7 , both containing Re^{7+} . The host glass composition selected is based on the AN-105 low-sulfur tank waste, one of the earliest glasses planned to be processed into LAW glass at Hanford and used in recent glass formulation melter studies of Tc retention.^{8,20} To avoid some of the known problems with different behavior noted for halide interaction with Re versus Tc,^{21,22} fluorine and chlorine were not included in the base glass composition for this study.

A process not common to oxide glass processing was intentionally employed in this study to reduce the volatilization potential of the rhenium salts from the melt during these experiments. This approach, while being drastically different from an actual melter scenario, was taken to avoid the experimental artifacts associated with measuring the solubility of volatile components. Here, glass powder was added to a fused quartz ampoule that was subsequently vacuum-sealed prior to heat treatment (Fig. 1). The ampoule provided an enclosure to reduce the loss of volatile species from the glass to the atmosphere during melting where the volatile vapors were still confined in the headspace above the melt. This special configuration was designed to determine the solubility of rhenium in this glass, as discussed elsewhere.^{23,24}

Once melted, the glass was air quenched, mounted in resin, cross-sectioned, and characterized. Several different techniques were employed to characterize the glass structure and the crystalline inclusions within the glass. These techniques included: X-ray diffraction (XRD), scanning electron microscopy (SEM), energy dispersive spectroscopy (EDS), electron probe microanalysis with wavelength dispersive spectroscopy (EPMA-WDS), differential scanning calorimetry, X-ray absorption near-edge structure (XANES) spectroscopy, magic-angle spinning nuclear magnetic resonance spectroscopy

C. Jantzen—contributing editor

Manuscript No. 32200. Received October 17, 2012; approved February 11, 2013.

^{*}Member, The American Ceramic Society

[†]Author to whom correspondence should be addressed. e-mail: brian.riley@pnl.gov

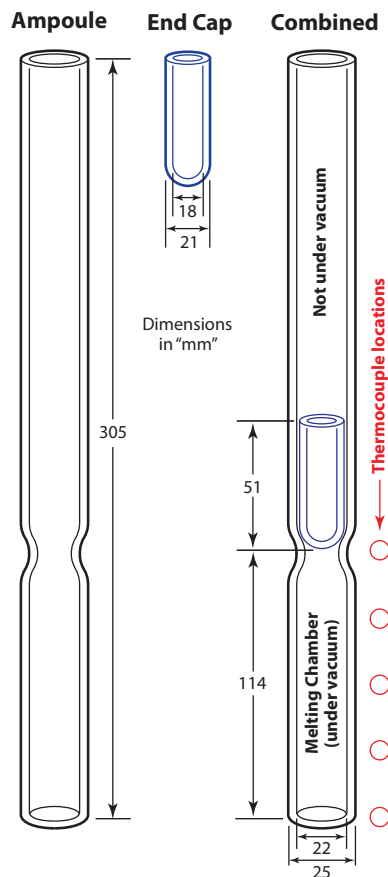


Fig. 1. Schematic of sealed fused quartz ampoule for glassmelting (dimensions are in mm). The glass batch is placed in the bottom portion of the combined ampoule on the right. The ampoule is open at the top and sealed at the bottom.

copy, Fourier transform infrared spectroscopy, Raman spectroscopy, laser ablation inductively coupled plasma mass spectroscopy (LA-ICP-MS), and inductively coupled plasma optical emission spectroscopy (ICP-OES). The methods and results from the XANES, ICP-OES, and some XRD as well as detailed discussion of the rhenium solubility in this glass are presented in prior publications.^{23,24} Here, we discuss the results from the XRD, SEM-EDS, EPMA-WDS, and LA-ICP-MS characterizations.

II. Experimental Procedure

(1) Glass Synthesis

The borosilicate LAW glass with nominal composition shown in Table I was synthesized with the melt-quenching technique and is termed the *baseline glass*. The baseline glass, or the glass without any Re^{7+} additions, was made in a large batch from the appropriate amount of oxides (MgO , Al_2O_3 , SiO_2 , Cr_2O_3 , ZrO_2 , TiO_2 , ZnO , Fe_2O_3), carbonates (CaCO_3 , Na_2CO_3 , K_2CO_3), H_3BO_3 , and Na_2SO_4 . The glass batch was homogenized in a vibrating agate mill and melted in a Pt/10%Rh crucible at 1200°C for 1 h in a Deltech furnace (Deltech, Inc.; Denver, CO). The resulting glass was quenched on an inconel plate and crushed inside a tungsten carbide mill within a vibratory mixer yielding a fine glass powder ($<40\ \mu\text{m}$) to homogenize it further.

The rhenium sources used were KReO_4 (Alfa Aesar, Ward Hill, MA, 99% metal basis) and Re_2O_7 (NOAH Tech., 99.99%,

-4 mesh). The target concentration of Re^{7+} added to the baseline glass was varied between 0 and 10000 ppm (see Table I), defined as parts per million of Re atoms in the glass (by mass). The fractions of the other components in

the glasses with Re additions were kept in constant ratios with those in the baseline glass, but renormalized to the remaining mass fraction after accounting for the Re source.

The LAW glass powder obtained from the aforementioned procedure and the specified amount of Re source powder were mixed in the tungsten carbide mill for a total mass of 30 g for each experiment. The glass frit was prepared this way so that the Re source powder was well mixed within the glass and captured by the glass powder during sintering at the maximum allowable solubility. It should be noted that the baseline glass was also remelted under similar conditions to the Re experiments (i.e., 1000°C , see below).

Each batch of glass powder (30 g) was placed into a flat-bottomed fused quartz tube and a fused quartz end cap was inserted into the tube (Fig. 1). The tube was then connected to a vacuum system with a compression fitting and evacuated. Once the pressure was $\sim 10^{-4}$ Pa, the tube was sealed with an oxygen-propane torch. This vacuum-sealed tube will hereafter be referred to as the ampoule. After sealing, five type-K thermocouples (OMEGA, Stamford, CN) were connected to the outside of the ampoule with stainless steel wire for temperature monitoring during the heat treatment. The ampoule was then inserted into a Deltech furnace preheated at 700°C . The temperature of the furnace was increased from 700°C to 1000°C at a heating rate of $5^\circ\text{C}/\text{min}$, followed by a dwell of 2 h at 1000°C , after which, the ampoule containing the glassmelt was quenched in air within a stainless steel canister.

(2) Sample Preparation for Analysis

To keep the entire sample intact during cutting and polishing, it was placed into a larger fused quartz container and vacuum impregnated with LR WhiteTM resin (SPI, West Chester, PA). Following this, the resin-impregnated samples were placed into a pressure chamber (Allied High Tech, Rancho Dominguez, CA) and filled with nitrogen gas to 3×10^5 Pa to further force the resin into the cracks and voids. The chamber was then placed in an oven so the resin could cure. The best results were obtained when the samples were baked at 40°C for 24 h, at 50°C for 24 h, and then at 60°C for 24 h all while inside the pressure chamber. Some cracking and shrinkage were observed in the resin after heat curing, but these voids were backfilled with an EpoThin resin (Buehler, Lake Bluff, IL). Once impregnated with resin, samples were cut longitudinally with a diamond wire saw (CT400, Diamond Wire Technology, LLC, Colorado Springs, CO) to remove a section $\sim 1/4$ inch thick from the center of the ingot. Samples were then polished with an LP-01 Syntron vibratory polisher (FMC Technologies, Saltillo, MS) to a $<1\ \mu\text{m}$ finish.

(3) X-Ray Diffraction

All of the glasses and selected crystalline samples were analyzed with a Bruker[®] D8 Advance (Bruker AXS Inc., Madison, WI) XRD with $\text{Cu K}\alpha$ emission ($\lambda = 1.5418\ \text{\AA}$). The detector used was a LynxEyeTM position-sensitive detector with a collection window of $3^\circ 2\theta$. Scan parameters for the salt phase were 5° – $70^\circ 2\theta$ with a step of $0.015^\circ 2\theta$ and a 0.3-s dwell at each step. To obtain better counting statistics for resolving the phases in the glass, a step of $0.009^\circ 2\theta$ was used with a 1-s dwell at each step. Bruker AXS DIF-FRAC^{plus} EVA was used to identify the crystalline phases present in the glasses.

(4) SEM and EDS

The microstructure was analyzed on polished and fractured surfaces from select samples with an SEM (JSM-5900, JEOL USA, Inc., Peabody, MA) equipped with a tungsten filament

Table I. Glass Compositions (Oxide Basis)

Target Re-conc. (ppm)	Unit	SiO ₂	Al ₂ O ₃	B ₂ O ₃	Na ₂ O	CaO	Fe ₂ O ₃	Cr ₂ O ₃	K ₂ O	MgO	SO ₃	TiO ₂	ZnO	ZrO ₂	Re ₂ O ₇	KReO ₄	SUM
0 ("baseline")	Mass%	45.30	6.10	10.00	21.00	2.07	5.50	0.02	0.47	1.48	0.16	1.40	3.50	3.00	–	–	100.00
	Mol%	50.40	4.00	9.60	22.64	2.47	2.30	0.01	0.33	2.45	0.13	1.17	2.87	1.63	–	–	100.00
100	Mass%	45.28	6.10	10.00	21.00	2.07	5.50	0.02	0.47	1.48	0.16	1.40	3.50	3.00	–	0.016	100.00
	Mol%	50.40	4.00	9.60	22.64	2.47	2.30	0.01	0.33	2.45	0.13	1.17	2.87	1.63	–	0.004	100.00
1000	Mass%	45.22	6.09	9.98	20.97	2.07	5.49	0.02	0.47	1.48	0.16	1.40	3.49	3.00	–	0.16	100.00
	Mol%	50.36	4.00	9.60	22.64	2.47	2.30	0.01	0.33	2.45	0.13	1.17	2.87	1.63	–	0.04	100.00
2500	Mass%	45.12	6.08	9.96	20.92	2.06	5.48	0.02	0.47	1.47	0.16	1.39	3.49	2.99	–	0.39	100.00
	Mol%	50.36	3.99	9.59	22.62	2.46	2.30	0.01	0.33	2.45	0.13	1.17	2.87	1.63	–	0.09	100.00
4000	Mass%	45.01	6.06	9.94	20.87	2.06	5.47	0.02	0.47	1.47	0.16	1.39	3.48	2.98	–	0.62	100.00
	Mol%	50.33	3.99	9.59	22.61	2.46	2.30	0.01	0.33	2.45	0.13	1.17	2.87	1.62	–	0.14	100.00
6415	Mass%	44.83	6.04	9.90	20.79	2.05	5.45	0.02	0.47	1.47	0.16	1.39	3.47	2.97	–	0.99	100.00
	Mol%	50.27	3.99	9.58	22.59	2.46	2.30	0.01	0.33	2.45	0.13	1.17	2.87	1.62	–	0.23	100.00
10000	Mass%	44.60	6.01	9.84	20.67	2.04	5.41	0.02	0.46	1.46	0.16	1.38	3.45	2.95	–	1.55	100.00
	Mol%	50.22	3.98	9.56	22.56	2.46	2.29	0.01	0.33	2.45	0.13	1.17	2.86	1.62	–	0.36	100.00
6407	Mass%	44.91	6.05	9.92	20.83	2.05	5.45	0.02	0.47	1.47	0.16	1.39	3.47	2.98	0.83	–	100.00
	Mol%	50.33	3.99	9.59	22.62	2.46	2.30	0.01	0.33	2.45	0.13	1.17	2.87	1.63	0.12	–	100.00

and a Robinson backscattered electron detector. A silicon drift detector was used to conduct EDS (Apollo XL, AMETEK, Berwyn, PA) for elemental dot mapping.

(5) EPMA and WDS

A JEOL JXA-8530F HyperProbe EPMA with a field-emission gun and five WDS's was used to quantify the spatial distribution of rhenium on polished samples from select glasses. The electron beam was set at an accelerating voltage of 20 keV and a current of 20 nA. Metallic Re (99.9% Re; Ted Pella, Inc., Redding, CA) was used as the standard for Re quantitative analysis. Because of the overlap in the X-ray energy lines for Si, Zn, and Re, special precautions were taken by quantifying Re with the $M_{\beta 1}$ peak (1.906 keV). These specific experimental conditions restricted the detection limit of Re to a minimum of ~336 ppm, thus glasses with target Re concentrations of <1000 ppm were not analyzed with EPMA-WDS.

Quantification utilized a ZAF data reduction routine (EPMA Analysis, JEOL) that corrected and quantified characteristic X-ray yields against mineral standards (Geller Microanalytical Laboratory, Inc., Topsfield, MA). The specific standards were as follows: SiO₂ for Si, corundum (Al₂O₃) for Al, rutile (TiO₂) for Ti, orthoclase (KAlSi₃O₈) for K, albite (NaAlSi₃O₈) for Na, metallic Zr for Zr, MgO for Mg, ZnS for Zn, wollastonite (CaSiO₃) for Ca, and hematite (Fe₂O₃) for Fe. Due to the uncertainty in the absorption of characteristic oxygen X-rays in the glasses, oxygen was not measured, but was calculated from oxide equivalents given the determined cations. Randomly selected regions of the glass were measured and the compositions were averaged. Rhenium inclusions were observed in various regions of the glass with Re^{7+} concentration of 6407 ppm (Re₂O₇) and were also measured. In addition, line scans were conducted on some of the samples in a probe mode with 256 pixels. The dwell time per pixel was set at 500 ms for a 1- μ m pixel size.

(6) LA-ICP-MS

A LA-ICP-MS was used to analyze the chemical nature of polished bulk glass samples and to detect the presence of any crystalline Re inclusions in the samples. The polished glass samples were mounted in a laser system sample holder (UP-266 Macro, New Wave Research, Inc., Portland, OR) and coupled to a quadrupole ICP-MS (PQ Excell, VG Elemental, England). The sensitivity for ¹⁸⁷Re was ~1000 counts per second per ppm (cps/ppm), based on a raster ablation with a 20- μ m diameter laser spot, rising to ~8200 cps/ppm with a 70- μ m diameter laser ablation spot. These values were

determined by ablating the National Institute of Standards and Technology "50 ppm" trace elements in a standard reference material (SRM) 612 glass.²⁵ In addition, comparative measurements were made with the "500 ppm" trace elements in glass standard SRM 610.²⁵ These standards are not certified for Re concentration, but have been measured by dissolution methods and reported in the literature, with SRM 612 having 6.57 ± 0.07 ppm Re content and SRM glass number 610 having 49.9 ± 0.3 ppm Re content.²⁶ Although it has been reported²⁷ that the Re concentration in the standards displays some local heterogeneity, this was minimized using the averaged Re signal intensity while the laser ablated an area ~2 mm \times 2 mm, so the ablation area was much larger than any local inhomogeneity in Re concentration.

Rhenium distribution studies on the fabricated glasses were performed by ablating a grid of 100 spots, typically 0.5 mm \times 0.5 mm total area, repeating the measurement over five to six sites across a sample and averaging the data. During Re analysis, the laser was scanned over the surface of the sample in a raster pattern (scan speed 25 μ m/sec) for a period >3 min while the ICP-MS collected the intensities of target analytes averaged over three 1-minute blocks. Similar laser ablation measurements were performed on the SRM 612 and/or SRM 610 standards under identical conditions, and the Re levels in the test glasses were estimated by relative signal ratios assuming the reported Re concentration in these standards as stated above. These SRM glasses were run before, and often in the midst of, the experimental glasses each day that the LA-ICP-MS was run to account for variations in set up, laser power drift, and other uncontrolled factors.

Single point feature studies, such as probing intact gas bubbles, were performed by allowing the laser to ablate into the glass to reach the subsurface features of interest. For these types of analysis, the ICP-MS was run in time-resolved analysis mode and is referred to here as depth profiling. Depth profiling with time-resolved LA-ICP was performed on a polished glass surface downward into the bulk of the sample as shown in Fig. 2. The experiment was conducted with a single laser spot (240 μ m diameter) using 100% powder and a 10 Hz repetition rate over 200 s. The subsurface air bubbles present in the glass were also penetrated by the laser beam to confirm the possible existence of rhenium in or around them.

III. Results and Discussion

(1) Visual Examination

The quenched samples were very fragile and, in all cases, the glass cracked upon cooling due to thermal stresses, but remained loosely intact as a single bulk piece. The LR

WhiteTM resin worked very effectively at keeping these samples intact for subsequent cutting and polishing. This resin provided three important advantages over other resins that we evaluated and later abandoned: (1) it was exceptional at penetrating the voids (attributed to its low viscosity), (2) it did not inadvertently cure during the vacuum impregnation process because it requires heat to cure when uncatalyzed, and (3) it did not dissolve the rhenium salts on the top of the samples. This resin is recommended for future work with similar experiments, especially where salt phases are of interest and dissolution in the potting material is a concern.

At melt temperatures in the 6415 ppm Re^{7+} (KReO_4) sample, a separate low viscosity liquid phase was observed, with an estimated viscosity similar to water at <0.1 Pa s. This phase floated on top of the glass surface and gradually solidified to a white-colored coating (Fig. 3). This phase did not appear to crystallize until the glass was rather cool ($\leq 500^\circ\text{C}$), estimated based on color of the glass, and well below the processing temperature of the melt (1000°C). This is consistent with the melting temperatures for these salts in the literature, presented in Table II.^{3,28–33} Detailed descriptions of the visual

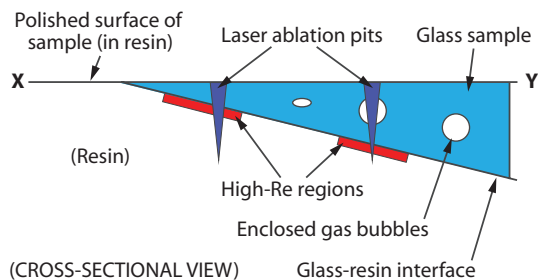


Fig. 2. Schematic of laser ablation depth profiling through bubbles.

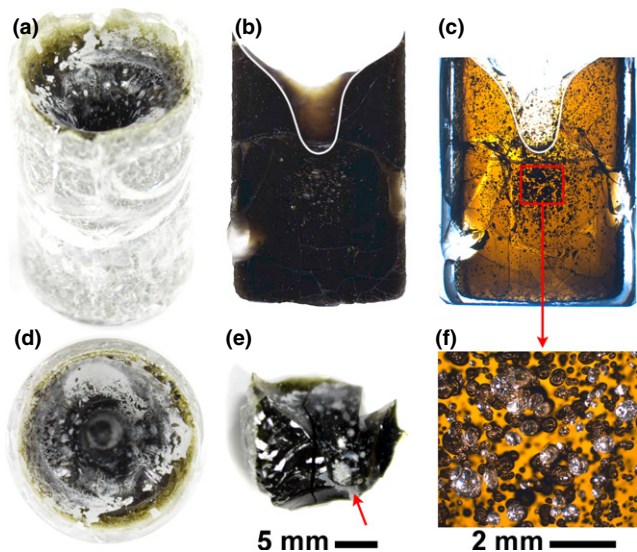


Fig. 3. (a–d) Photographs and (f) optical micrograph of 6415 ppm Re^{7+} (KReO_4) sample, as well as (e) photograph of fractured specimen surface from the 6407 ppm Re^{7+} (Re_2O_7) sample. A white line is added in (b) and (c) as a guide to the eye showing the outline of the dimple through the center line of the ingot. The oblique (a), cross-sectional (b, c), and top (d) views provide a better understanding of the appearance of these ingots. The box in (c) is enlarged in (f) where the lightly colored bubbles in (f) are open on the polished surface. The white residue in (a), (d), and (e) is alkali rhenium oxide salts. Scale bars are included for micrographs that are not obvious (ingot width is 22 mm, and 25 mm with fused quartz ampoule).

appearance of these various glasses have been presented previously.³⁴

Representative pictures for glasses produced by this process are presented in Fig. 3 for the 6415 ppm Re^{7+} (KReO_4) sample and the 6407 ppm Re^{7+} (Re_2O_7) sample. The oblique view in Fig. 3(a) shows the presence of the shattered fused quartz ampoule surrounding the glass ingot. The ampoule cracked because of the thermal expansion mismatch between the glass and fused quartz. Pictures of a cross-section can be found in Fig. 3(b) (reflected light) and Fig. 3(c) (transmitted light); a white line is present on both of the cross-sections to show the outline of the dimple present through the center line of the ingot. The top view (Fig. 3(d)) shows the presence of the white salt phase on top of the black glass. The broken piece from the 6407 ppm Re^{7+} (Re_2O_7) in Fig. 3(e) shows the distinction between salt-covered surfaces that were on the top and those that were fractured from the bulk glass upon cooling (see arrow). It is on the fractured glass surfaces of this sample that the dendritic, phase-separated sulfate and perrhenate phases were found (described later). It can be clearly seen from Figs. 3(c) and (f) that the center of the ingot is full of bubbles.

(2) Crystallinity in Re Glasses

(A) XRD: Most of the samples were X-ray amorphous as analyzed in bulk form, with the exception of a few small diffraction peaks in the 6407 ppm Re^{7+} (Re_2O_7) and 10000 ppm Re^{7+} (KReO_4) samples that were attributed to alkali perrhenates (see Fig. 4(a) and McCloy *et al.*,^{23,24} respectively). The white powders (salt phase) observed with the KReO_4 samples at ≥ 6400 ppm Re^{7+} loadings were composed of alkali perrhenates and cristobalite-high, whereas the salt from the Re_2O_7 experiment with 6407 ppm Re^{7+} was composed of $(\text{Na,K})_2\text{SO}_4$ and NaReO_4 (note that KReO_4 was not observed) [Fig. 4(b)]. However, based on SEM-EDS results (presented below), K was observed to interact with Re (likely as KReO_4) in some cases.

The 10000 ppm Re^{7+} sample was cut into three sections (top, middle, and bottom) for XRD analysis and each section was analyzed separately to assess the distribution of the insoluble Re species. The regions closer to the top surface of the ingot showed increasing crystalline content with a heterogeneous distribution of alkali perrhenate inclusions (more details are provided elsewhere^{23,24}).

(B) LA-ICP-MS: No significant interfacial reactions between the glass and the walls of quartz ampoule were observed with LA-ICP-MS (not shown). In agreement with the XRD results (Fig. 4), the presence of Re-rich crystalline inclusions in the 6407 ppm Re^{7+} glass (Re_2O_7) was confirmed with LA-ICP-MS data as presented in Fig. 5(a). A sharp increase in the intensity counts for ^{187}Re in Fig. 5(a) implies that the laser beam ablated a Re-containing crystalline inclusion that was likely in the form of NaReO_4 as detected by XRD analysis (Fig. 4).

Figure 5(b) shows the depth profile LA-ICP data from the 6407 ppm Re^{7+} glass (Re_2O_7) confirming the presence of an inclusion in the bulk of glass sample. This inclusion was visible as a white material under the surface of the glass. Similar observations were also recorded on powders of the glass with 10000 ppm Re^{7+} . The air bubbles present in the glass [see

Table II. Melting Temperatures (T_m) for the Rhenium and Sulfate Salts Observed Here^{3,28–33}

Salt	T_m ($^\circ\text{C}$)	References
KReO_4	550–555	3,28,32
K_2SO_4	1069	33
NaReO_4	~300–420	3,28,32
Na_2SO_4	884	33
Re_2O_7	220–300.3	3,28–31

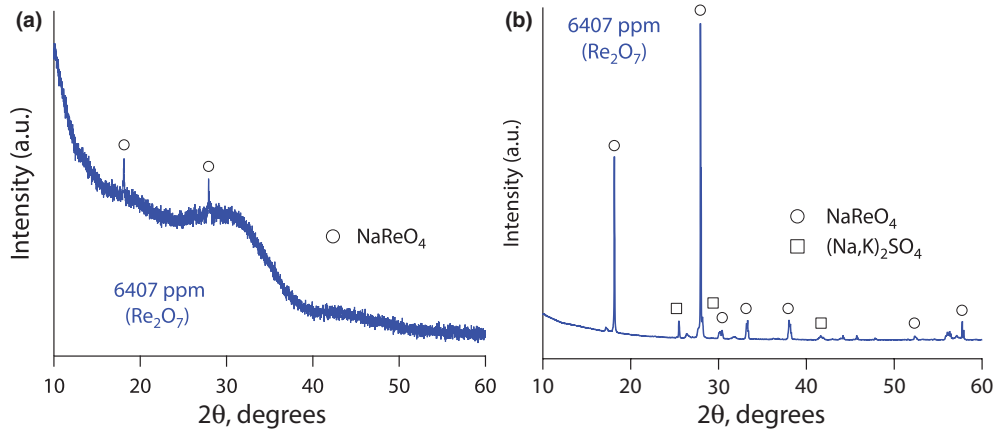


Fig. 4. Powder XRD of (a) the glass and (b) the white powder residue on the surface of the 6407 ppm Re^{7+} (Re_2O_7) sample.

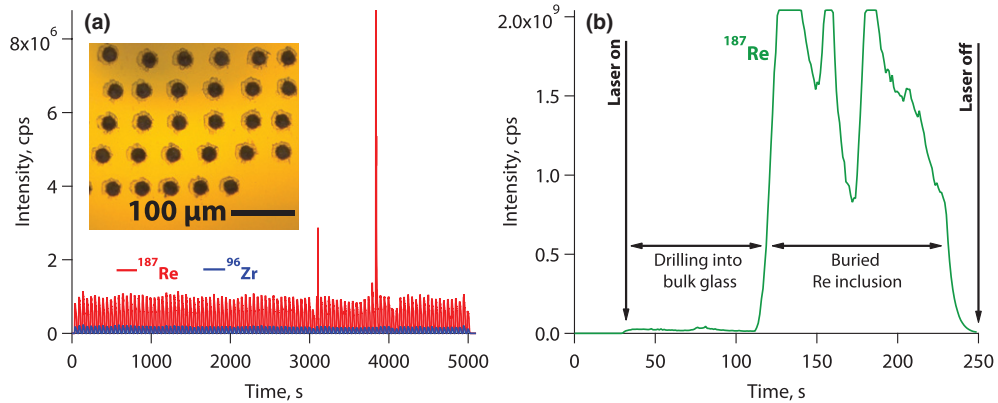


Fig. 5. (a) LA-ICP-MS signal versus time showing the presence of ^{187}Re inclusions in the 6407 ppm Re^{7+} glass (Re_2O_7) where the inset shows a typical ablation pattern. A spectrum for ^{96}Zr is included for comparison as a background signal (very low counts). (b) Depth profiling of a white inclusion in the 6407 ppm Re^{7+} glass (Re_2O_7) shows that the ^{187}Re signal saturates the detector while it is in the bulk of the inclusion, then returns to background when the whole inclusion is ablated.

Figs. 3 (c) and (f)] were also targeted by the laser beam to confirm the possible existence of rhenium in or around them. No rhenium was found, confirming their identity as air bubbles and not as trapped Re vapor.

The initial motivation for using LA-ICP-MS was to see if a segregated phase was present on the specimen surface or subsurface using depth profiling, in conjunction with an optical microscope. Previous reports showed that Re could concentrate in reduced metallic form within silicate melts as “micronuggets” and artificially inflate solubility limits.³⁵ Although this study did find evidence of (Na,K)ReO₄ inclusions, no evidence was found of these micronuggets. The redox was subsequently measured for these glasses and was determined to be $\text{Fe}^{2+}/\text{Fe}_{\text{tot}} \lesssim 0.1$ by an independent laboratory (in the redox analysis, Fe^{2+} was analyzed colorimetrically using phenanthroline, and Fe_{tot} was analyzed using ICP). Therefore, the tendency of Re to reduce would be less likely to occur in our samples due to the conditions present in the reaction vessel.³⁶ Inclusions containing Re in the samples from this study were indicated by very large excursions of Re concentration and were very spatially confined, which is different from the heterogeneous Re distribution reported for reduced Re elsewhere.³⁵

(C) SEM and EDS: The SEM micrographs of the white powder from the 6407 ppm Re^{7+} sample (Re_2O_7) at different locations on the glass surface illustrate their highly crystalline microstructure and dendritic morphology (Fig. 6). The EDS elemental dot map of the dendritic crystals found on a fracture surface revealed the dominance of sodium, sulfur, and rhenium in these crystals (Fig. 7). Although the crystalline microstructure of the white powders is enriched in

sulfur along with Re and Na, we did not observe any Re–S containing phase with XRD analysis [Fig. 4(b)].

In addition, EDS confirmed that the sulfur in the 6407 ppm Re^{7+} (Re_2O_7) sample was associated with sodium (probably Na_2SO_4 with some K), whereas the rhenium appeared to be mostly associated with potassium (probably KReO_4 with some Na). This is different from the XRD data presented above where only NaReO_4 was observed in the bulk XRD spectrum, but the combined techniques show that both NaReO_4 and KReO_4 exist, which is in agreement with the 10000 ppm Re sample. It is likely that the perrhenate and sulfate salts were intimately mixed in the low viscosity liquid on top of the glass and then deposited in the cracks upon cooling where they crystallized into separate phases. As the viscosity of the molten salts is extremely low compared with the glass and these salts are miscible with one another, they are expected to be intermixed during the melting process. Because of the morphology of the dendritic sulfate phase, we know that the salts separately crystallize at a low temperature, but the eutectic of the mixed salt was not determined.

Energy dispersive spectroscopy was found not to be a reliable technique for semiquantitative Re determination. Firstly, peak overlap was an issue between Si, Zn, and Re. The baseline glass contained both Si ($K_\alpha = 1.739$ keV) and Zn ($K_\alpha = 8.628$ keV), which have X-ray emission energies comparable to Re M_α (1.842 keV) and L_α (8.650 keV) X-rays, respectively. Also, the Re concentrations in these glasses were near or below the reliable detection limit for EDS. For this reason, a limited number of samples were investigated with EPMA-WDS, which has a much higher energy resolution

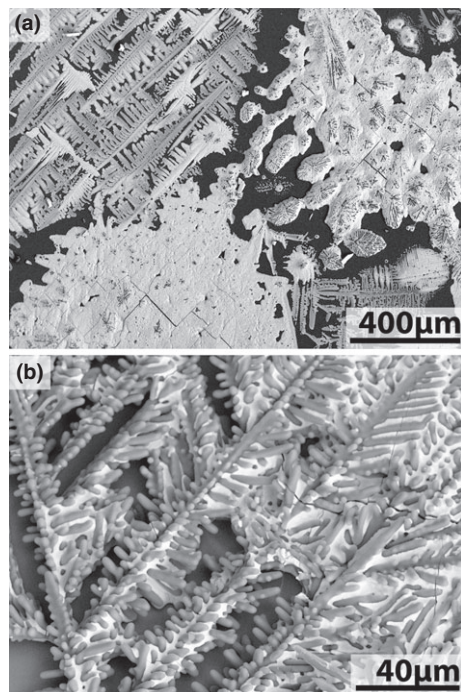


Fig. 6. SEM micrographs of salt phase on (a) the top and (b) on a fracture surface of the Re_2O_7 glass.

and is suitable for quantitative analysis given appropriate standards.

(D) *EPMA with WDS*: The 1000 ppm and 6415 ppm Re^{7+} (KReO_4) samples were measured with EPMA-WDS and the values were 8×10^2 and 1.8×10^3 ppm Re, respectively. These values are lower than the Re concentrations determined by ICP-OES previously.^{23,24} In this work, Re in the glass is a trace element, whereas the Re metal standard was 99.9% Re. The matrix effects of Z (atomic number), A (absorption), and F (fluorescence), or ZAF, for the sample and standard are significantly different, which can lead to the error in results. For the WDS quantitative analysis, the composition of the standard was used to calculate the ZAF; the concentration of the element in the unknown sample (C) was calculated by $C/C_{\text{std}} = [\text{ZAF}] I/I_{\text{std}}$, where I/I_{std} is the count ratio of the sample to the standard and C_{std} is the concentration of the standard. When the sample and the standard have similar composition, their ZAF correction is similar, but, when the sample and standard have very different compositions, as in this case, the calculated ZAF can be very different from the actual ZAF of the sample. In addition, Na volatilization due to electron-induced damage further made quantification unreliable.

Figure 8 shows a line scan across the 6415 ppm Re^{7+} (KReO_4) glass where a Re-containing inclusion was present at the interface between the glass and the fused quartz wall.

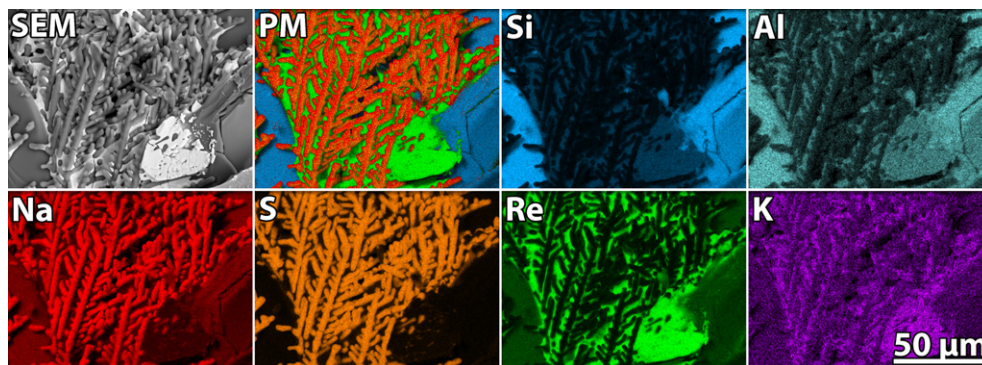


Fig. 7. Backscattered electron SEM micrograph, phase map (PM), and elemental dot maps (Si, Al, Na, S, Re, and K) for dendritic crystals found on the fracture surface of the Re_2O_7 glass (based on results from EDS analysis).

No other inclusions were found in the bulk of this sample with EPMA or XRD and the formation mechanism for this isolated particle is not currently known. Compared with LA-ICP-MS, the backscattered electron detector on the EPMA provides atomic number contrast and provides visualization of Re-containing areas against the surrounding glassy matrix. The LA-ICP-MS utilizes an optical microscope to visualize the sampling region, often making it difficult to distinguish between the glass and the salt inclusions.

(3) Rhenium Solubility

The XRD results combined with the visual observations of the molten salt layer allow classification of these glasses using the parlance of Jantzen *et al.*¹⁵ in terms of the degree of saturation. *Undersaturated* systems (including melt, salt, and gas above melt) do not have any appearance of molten salt (gall) or inclusions and this category includes 100, 1000, and 4000 ppm Re^{7+} (KReO_4) glasses. The 6415 ppm target Re^{7+} (KReO_4) glass must be described as oversaturated, as a molten salt phase was observed but XRD could not detect any Re-containing phases (although they might exist below the XRD detection limit). The 6407 ppm Re^{7+} (Re_2O_7) and the 10000 ppm Re^{7+} (KReO_4) glasses are classified as *supersaturated*, as they had both a gall phase and Re-containing inclusions present as alkali perrhenates. Note that the 4000 ppm glass, though classified as undersaturated in this way, did not fully incorporate all the Re as the overall solubility of Re^{7+} has been determined to be ~ 3000 ppm.²³ The rest of the Re in this case was presumably lost to volatilization and condensed on the ampoule wall above the melt.

Volatilization can occur by different methods depending on various process details,¹⁵ including temperature, glass composition (particularly alkali, but also possibly boron, which may influence alkali distribution),³⁷ redox equilibrium, and pressure of the volatile species (e.g., SO_2 for sulfur and possibly Re_2O_7 for rhenium). The pressure of the volatile species is influenced not only by the degree of saturation but also by the specific experimental conditions, whereby a closed system (such as our ampoule) favors suppression of the volatilization, thus increasing the perceived solubility.¹⁵ For example, Jantzen *et al.*¹⁵ previously found via meta-analysis of previously published data that an increased alkali content increased the measured solubility of sulfate, and that glasses supersaturated with sulfate (e.g., with sulfur-containing surface salts and glass inclusions) showed a higher apparent sulfur solubility than comparable to ones with lower sulfur targets.

However, determining solubility in the context of glasses with inclusions is difficult if proper experimental precautions are not taken, such as grinding and washing the glass powder to remove the water-soluble salt phase inclusions. A robust assessment of these matters must include a mass balance of the target components and the results of this for our rhenium-containing glass are a subject of a future communication. The results of our mass balance studies, to be reported

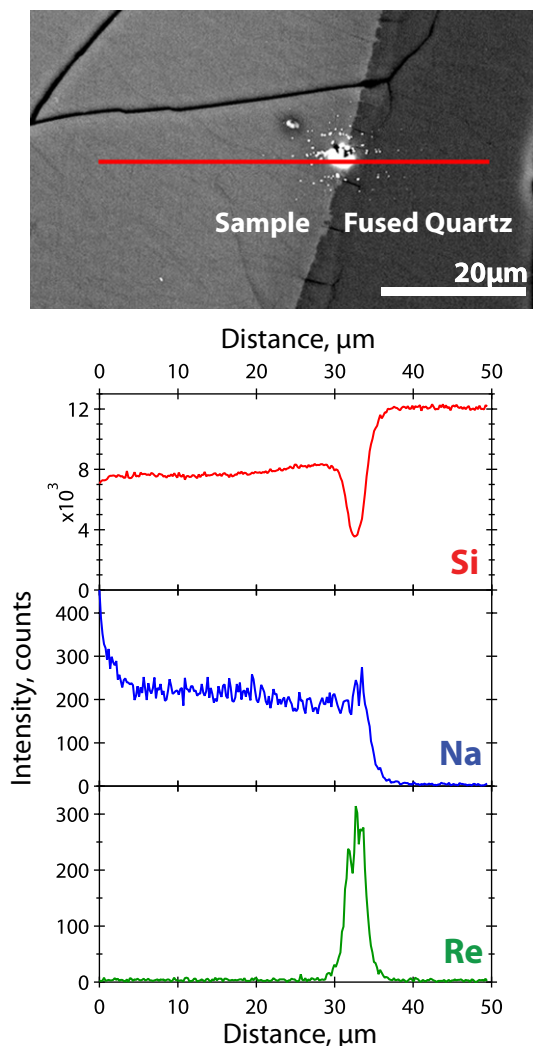


Fig. 8. (top) Backscattered electron EPMA micrograph (see line on micrograph at top) showing a Re inclusion as a brighter phase than the surrounding sample and the fused quartz wall. (bottom) WDS line scan showing the Si, Na, and Re distribution in the region denoted by the line in the above micrograph.

separately, indicate that sulfur is clearly present in the phase (s) that volatilized and redeposited on the ampoule wall above the glass as well as in the rinse of the powdered glass ingot (dissolving any surface salt/gall as well as any salt inclusions). However, sulfur was present at a much lower level than Re, despite sulfur being present at levels well below its solubility. These results suggest that rhenium is having an effect on the transport and volatilization of sulfur. Similar collective effects are expected with other salt-forming components of yellow phase (e.g., chromate, molybdate, pertechnetate).³⁴

It should be stressed that the Re solubility in our case, of ~3000 ppm, was determined by dissolution (ICP-OES) based on an average of the maximum measured Re concentration of three KReO_4 source glasses²³: an undersaturated glass (4000 ppm target), an oversaturated glass (6415 ppm target), and a supersaturated glass (10000 ppm target). The replicates for the supersaturated glass showed bimodal distribution (i.e., some Re concentrations >3000 ppm), indicative of some glass pieces containing crystalline Re inclusions (higher Re apparent concentration) with others being very similar in concentration to the assessed solubility (~3000 ppm). The glass pieces used for dissolution did not contain the gall layer. These data have been presented previously by McCloy *et al.*,²³ but not previously discussed in this way.

As discussed in previous work,^{19,20} the valence of the rhenium incorporated into the glass structure was determined for the 100, 1000, 6415, and 10000 ppm Re^{7+} (KReO_4) specimens with Re-XANES and, for all specimens, all of the Re was found as Re^{7+} within experimental error. As previously stated, it is expected that the measured solubility will be influenced by factors that were not determined in this study, such as alkali and boron concentration, melt temperature, and melt redox. As Re^{4+} is much more difficult to prepare than the Tc^{4+} of real interest, the study on redox was reserved for the Tc solubility study, which is currently underway.

Some caveats must accompany the data presented here. First, the goal of this study was to determine the solubility of technetium in this glass and a rhenium surrogate was used that will not behave exactly like technetium in a real melter scenario; the data discussed here were presented for instructional purposes to prepare for future experiments with technetium (currently underway). One of the primary differences between Re^{7+} and Tc^{7+} present in a melt exposed to air is that Re will tend to remain as Re^{7+} and some Tc may reduce to Tc^{4+} . Second, these experiments are not intended to be directly compared with those run in open crucibles or in glass melters because of redox differences. Rather, our experimental approach allowed for supersaturation of rhenium above the solubility limit, which, upon quenching, resulted in the gall layer for glasses with Re loadings >4000 ppm. The intent of this study was to quantify the upper solubility of rhenium in oxidizing melt conditions by allowing the melt to supersaturate. The result of supersaturation is the formation of a Re-containing gall layer and bulk crystals of alkali perrhenate as described herein. Thus, we show that the behavior of Re in borosilicate glasses is similar to that observed with sulfur and molybdenum with the formation of a molten salt phase and crystallization of alkali salts.^{15–19}

IV. Conclusions

A series of sodium borosilicate glasses were produced with increasing concentrations of Re^{7+} up to 10000 ppm Re (by mass), added as either KReO_4 or Re_2O_7 . Rhenium inclusions were observed in 6407 ppm Re^{7+} (Re_2O_7) and 10000 ppm Re^{7+} (KReO_4) samples. A white salt layer was found on the top of three samples (these aforementioned two and the 6415 ppm Re^{7+} with KReO_4) and was determined to be a mixture of $(\text{Na,K})\text{ReO}_4$ and $(\text{Na,K})_2\text{SO}_4$. Several techniques were used to identify and characterize these salts and inclusions. In the 6407 ppm Re^{7+} (Re_2O_7) sample, salts were observed on the glass fracture surfaces that showed salts of K and Na sulfates and perrhenates suggesting that they were a single phase in liquid form that crystallized out as distinct phases. These results show that the sulfate concentration is important for ReO_4^- (and, by extension, TcO_4^-) crystallization, even at low concentrations. The relationship between the composition and concentration of these anions and the retention of technetium in nuclear waste glass remains unclear. These results demonstrate the need for a more developed understanding of the retention issues with Tc during the vitrification process so it can be managed appropriately.

Acknowledgments

This work was supported by the Department of Energy's Waste Treatment & Immobilization Plant Federal Project Engineering Division. The authors thank Orville (Tom) Farmer III for consultation regarding LA-ICP-MS, Clyde Chamberlin for helping prepare the samples, and Jarrod Crum for comments on the study. Pacific Northwest National Laboratory is operated by Battelle Memorial Institute for the U.S. Department of Energy under contract DE-AC05-76RL01830. A portion of this work was conducted at the Environmental Molecular Science Laboratory, a national scientific user facility sponsored by the Department of Energy's DOE Office of Biological and Environmental Research, located at PNNL.

References

- ¹F. Mann, "Annual Summary of the Integrated Facility Performance Assessment for 2004"; DOE/ORP-2000-19, Rev. 4, CH2M HILL Hanford Group, Inc., Richland, WA, 2004.
- ²J. H. Westsik, "Hanford Site Secondary Waste Roadmap"; PNNL-18196. Pacific Northwest National Laboratory, Richland, WA, 2009.
- ³J. G. Darab and P. A. Smith, "Chemistry of Technetium and Rhenium Species During Low-Level Radioactive Waste Vitrification," *Chem. Mater.*, **8** [5] 1004–21 (1996).
- ⁴R. E. Meyer, W. D. Arnold, F. I. Case, and G. D. O'Kelley, "Solubilities of Tc(IV) Oxides," *Radiochim. Acta*, **55**, 11–8 (1991).
- ⁵G. Shaw, "Radioactivity in the Terrestrial Environment," Radioactivity in the Environment, Vol. 10, Elsevier, Oxford, UK, 2005.
- ⁶W. Um, H.-S. Chang, J. P. Icenhower, W. W. Lukens, R. J. Serne, N. P. Qafoku, J. H. Westsik, E. C. Buck, and S. C. Smith, "Immobilization of 99-Tc(IV) by Fe(II)-Goethite and Limited Reoxidation," *Environ. Sci. Technol.*, **45** [11] 4904–13 (2011).
- ⁷H. Lammertz, E. Merz, and S. Halaszovich, "Technetium Volatilization During HLLW Vitrification"; pp. 823–9, in *Proc. of the Mat. Res. Soc. Symp. Sci. Basis Nucl. Waste Manage. VIII*, Vol. 44, Edited by C. M. Jantzen, J. A. Stone and R. C. Ewing. Materials Research Society, Warrendale, PA, 1984.
- ⁸K. S. Matlack, I. S. Muller, I. L. Pegg, and I. Joseph, "Improved Technetium Retention in Hanford LAW Glass - Phase 1," VSL-10R1920-1. Vitreous State Laboratory, The Catholic University of America, Washington, D.C., 2010.
- ⁹D. S. Kim, C. Z. Soderquist, J. P. Icenhower, B. P. McGrail, R. D. Scheele, B. K. McNamara, L. M. Bagaasen, M. J. Schweiger, J. V. Crum, J. D. Yeager, J. Matyas, L. P. Darnell, H. T. Schaef, A. T. Owen, A. E. Kozelisky, L. A. Snow, and M. J. Steele, "Tc Reductant Chemistry and Crucible Melting Studies With Simulated Hanford Low-Activity Waste," PNNL-15131. Pacific Northwest National Laboratory, Richland, WA, 2005.
- ¹⁰R. Gales, J. Perez, B. MacIsaac, D. Siemer, and J. McCray, "Test Summary Report INEEL Sodium-Bearing Waste Vitrification Demonstration - RSM-01-1. PNNL-13522," Pacific Northwest National Laboratory, Richland, WA, 2001.
- ¹¹H. Li, P. Hrma, and J. D. Vienna, "Sulfate Retention in Simulated Radioactive Waste Borosilicate Glasses"; pp. 237–45, in *Proc. of the Env. Issues Waste Manage. Tech. Ceram. Nucl. Ind. VI*, Vol. 119, Edited by D. R. Spearing, G. L. Smith and R. L. Putnam. The American Ceramic Society, Westerville, OH, 2001.
- ¹²I. L. Pegg, H. Gan, I. S. Muller, D. McKeown, and K. Matlack, "Summary of Preliminary Results on Enhanced Sulfate Incorporation During Vitrification of LAW Feeds," VSL-00R3630-1. Vitreous State Laboratory, The Catholic University of America, Washington, D.C., 2001.
- ¹³P. Hrma, J. Vienna, and J. Ricklefs, "Mechanism of Sulfate Segregation During Glass Melting"; pp. 147–58, in *Proc. of the Mat. Res. Soc. Symp. - Sci. Basis Nucl. Waste Manage. XXVI*, Vol. 757, Edited by R. J. Finch and D. B. Bullen. Materials Research Society, Warrendale, PA, 2003.
- ¹⁴P. Hrma, J. Vienna, W. Buchmiller, and J. Ricklefs, "Sulfate Retention During Waste Glass Melting"; pp. 93–100, in *Proc. of the Env. Issues Waste Manage. Tech. Ceram. Nucl. Ind. IX - Ceram. Trans.*, Vol. 155, Edited by J. D. Vienna and D. R. Spearing. The American Ceramic Society, Westerville, OH, 2004.
- ¹⁵C. M. Jantzen, M. E. Smith, and D. K. Peeler, "Dependency of Sulfate Solubility on Melt Composition and Melt Polymerization"; pp. 141–52 in *Proc. of the Environmental Issues and Waste Management Technologies in the Ceramic and Nuclear Industries X*, Vol. 168, Edited by J. D. Vienna, C. C. Herman and S. Marra. The American Ceramic Society, Westerville, OH, 2005.
- ¹⁶D. Caurant, P. Loiseau, O. Majerus, V. Aubin-Chevaldonnet, I. Bardez, and A. Quintas, "Glasses, Glass-Ceramics and Ceramics for Immobilization of Highly Radioactive Nuclear Wastes," pp. 248–50. Nova Science Publishers, New York, 2009.
- ¹⁷G. Calas, M. Le Grand, L. Galois, and D. Ghaleb, "Structural Role of Molybdenum in Nuclear Glasses: An EXAFS Study," *J. Nucl. Mater.*, **322** [1] 15–20 (2003).
- ¹⁸G. N. Greaves, "EXAFS and the Structure of Glass," *J. Non-Cryst. Solids*, **71** [1–3] 203–17 (1985).
- ¹⁹R. K. Mishra, K. V. Sudarsan, P. Sengupta, R. K. Vatsa, A. K. Tyagi, C. P. Kaushik, D. Das, and K. Raj, "Role of Sulfate in Structural Modifications of Sodium Barium Borosilicate Glasses Developed for Nuclear Waste Immobilization," *J. Am. Ceram. Soc.*, **91** [12] 3903–7 (2008).
- ²⁰K. S. Matlack, I. Joseph, W. L. Gong, I. S. Muller, and I. L. Pegg, *Glass Formulation Development and DM10 Melter Testing With ORP LAW Glasses*. VSL-09R1510-2. Vitreous State Laboratory, The Catholic University of America, Washington, D.C., 2009.
- ²¹W. W. Lukens, D. K. Shuh, I. S. Muller, and D. A. McKeon, "X-ray Absorption Fine Structure Studies of Speciation of Technetium in Borosilicate Glasses"; pp. 101–6 in *Proc. of the Mat. Res. Soc. Symp.*, Vol. 802, Edited by J. Joyce, M. F. Nicol, D. Shuh, L. Soderholm, and J. G. Tobin. Materials Research Society, Warrendale, PA, 2004.
- ²²J. P. Icenhower, N. P. Qafoku, J. M. Zachara, and W. J. Martin, "The Biogeochemistry of Technetium: A Review of the Behavior of an Artificial Element in the Natural Environment," *Am. J. Sci.*, **310** [8] 721–52 (2010).
- ²³J. McCloy, B. J. Riley, A. Goel, M. Liezers, M. J. Schweiger, C. P. Rodriguez, P. R. Hrma, D.-S. Kim, W. W. Lukens, and A. A. Kruger, "Rhenium Solubility in Borosilicate Nuclear Waste Glass: Implications for the Processing and Immobilization of Technetium-99," *Environ. Sci. Technol.*, **46** [22] 12616–22 (2012).
- ²⁴J. McCloy, B. J. Riley, A. Goel, M. Liezers, M. J. Schweiger, C. P. Rodriguez, P. R. Hrma, D.-S. Kim, W. W. Lukens, and A. A. Kruger, "Rhenium Solubility in Borosilicate Nuclear Waste Glass: Implications for the Processing and Immobilization of Technetium-99"; PNNL-21553. Pacific Northwest National Laboratory, Richland, WA, 2012.
- ²⁵K. P. Jochum, U. Weis, B. Stoll, D. Kuzmin, Q. Yang, I. Raczek, D. E. Jacob, A. Stracke, K. Birbaum, D. A. Frick, D. Günther, and J. Enzweiler, "Determination of Reference Values for NIST SRM 610–617 Glasses Following ISO Guidelines," *Geostand. Geoanal. Res.*, **35** [4] 397–429 (2011).
- ²⁶P. J. Sylvester and S. M. Eggins, "Analysis of Re, Au, Pd, Pt and Rh in NIST Glass Certified Reference Materials and Natural Basalt Glasses by Laser Ablation ICP-MS," *Geostand. Newslett.*, **21** [2] 215–29 (1997).
- ²⁷S. M. Eggins and J. M. G. Shelley, "Compositional Heterogeneity in NIST SRM 610-617 Glasses," *Geostandard. Newslett.*, **26** [3] 269–86 (2002).
- ²⁸K. B. Lebedev, *The Chemistry of Rhenium*, pp. 5–24. Butterworth & Co. (Publishers) Ltd., London, 1962.
- ²⁹R. Colton, *The Chemistry of Rhenium and Technetium*, pp. 33–52. Interscience Publishers: John Wiley & Sons Ltd., New York, 1965.
- ³⁰E. Ogawa, "Vapour Pressure of Rhenium Heptoxide, Vapour Pressure and Dissociation Pressure of Rhenium Octoxide," *Bull. Chem. Soc. Jpn.*, **7** [8] 265–73 (1932).
- ³¹W. T. Smith Jr, L. E. Line Jr, and W. A. Bell, "The Vapor Pressures of Rhenium Heptoxide and Perrhenic Acid," *J. Am. Chem. Soc.*, **74** [19] 4964–6 (1954).
- ³²W. Lukas and M. Gaune-Escard, "Temperatures and Enthalpies of Melting of Alkali-Metal Perrhenates," *J. Chem. Thermodyn.*, **14** [6] 593–7 (1982).
- ³³A. C. Taş, "Molten Salt Synthesis of Calcium Hydroxyapatite Whiskers," *J. Am. Ceram. Soc.*, **84** [2] 295–300 (2001).
- ³⁴A. Goel, J. S. McCloy, C. F. Windisch Jr, B. J. Riley, M. J. Schweiger, C. P. Rodriguez, and J. M. F. Ferreira, "Structure of Rhenium-Containing Sodium Borosilicate Glass," *Int. J. Appl. Glass Sci.* DOI: 10.1111/ijag.12003 (2012).
- ³⁵W. Ertel, H. S. C. O'Neill, P. J. Sylvester, D. B. Dingwell, and B. Spettel, "The Solubility of Rhenium in Silicate Melts: Implications for the Geochemical Properties of Rhenium at High Temperatures," *Geochim. Cosmochim. Acta*, **65** [13] 2161–70 (2001).
- ³⁶W. W. Lukens, D. A. McKeown, A. C. Buechele, I. S. Muller, D. K. Shuh, and I. L. Pegg, "Dissimilar Behavior of Technetium and Rhenium in Borosilicate Waste Glass as Determined by X-ray Absorption Spectroscopy," *Chem. Mater.*, **19** [3] 559–66 (2007).
- ³⁷D. Caurant, O. Majerus, E. Fadel, A. Quintas, C. Gervais, T. Charpenier, and D. Neuville, "Structural Investigations of Borosilicate Glasses Containing MoO₃ by MAS NMR and Raman Spectroscopies," *J. Nucl. Mater.*, **396** [1] 94–101 (2010). □